KDM5D expression is lost in cisplatin-resistant neuroblastoma cells

NATALIA PODHORSKA, JAN HRABETA, MARIE BELHAJOVA and TOMAS ECKSCHLAGER

Department of Pediatric Hematology and Oncology, 2nd Faculty of Medicine, Charles University and Motol University Hospital, 150 06 Prague 5, Czech Republic

Received November 19, 2024; Accepted November 12, 2025

DOI: 10.3892/or.2026.9084

Abstract. Chemoresistance is a major cause of cancer therapy failure. Increasing evidence points to the importance of histone lysine demethylase function, whose dysregulation has been described in several types of cancer. KDM5, a family of histone lysine demethylases, may carry out a key role in the downregulation of tumor-suppressors or upregulation of oncogenes and in the development of drug tolerance. The present study examined the expression of KDM5D in cell lines derived from high-risk neuroblastoma. The present study found that KDM5D expression was lost in all cisplatin-chemoresistant neuroblastoma cell lines compared with sensitive parental cells. In addition, the cisplatin-chemoresistant neuroblastoma cell line had increased expression of the ubiquitin ligase cullinaA 4A (CUL4A) compared with the sensitive parental cells. CUL4A carries out a role in cellular processes and its aberrant regulation has been observed in a number of types of cancer. The present study shows that silencing of KDM5D causes a more aggressive phenotype of neuroblastoma by promoting cell proliferation and migration, evading cell death, promoting S phase of the cell cycle and desensitizing sensitive cells to cisplatin via the gene *CUL4A*. In addition, ectopic expression of KMD5D in a cisplatin-resistant cell line reversed these phenomena. The results suggest that KDM5D and/or CUL4A may be a biomarkers of chemoresistance to cisplatin and a potential therapeutic target in neuroblastoma.

Introduction

Covalent histone methylation of lysine residues carries out a key role in regulating chromatin dynamics and functions (1-3). Methylation of lysines on histone H3 and H4 activates or represses gene transcription, depending on the position of the modified residues (1,4). In general, methylated histone H3 lysine 4 (H3K4) is associated with active or balanced gene states, whereas methylated H3K9 and H3K27 are gene repressive (5). The removal of methyl groups from lysine residues on histones is regulated by histone lysine demethylases (KDM) (6,7).

To date, two distinct families of demethylases have been described the flavin-dependent KDM1 and the JmjC domain-containing KDM2-8 subfamilies. The first family, KDM1, catalyzes the demethylation of mono- and di-methylated lysine residues (Kme1 and Kme2). The second family of KDMs (KDM2-8) is capable of demethylating Kme1, Kme2 and Kme3 (8). In addition, KDMs demethylate non-histone substrates and also have several demethylase-independent functions (9). The KDM expression profile varies in different cells and tissues. Altered expression of KDMs, especially those targeting H3K4 and H3K27, is common in several types of human cancer (9). The KDM5 subfamily, that has 4 members (KDM5A-D), is capable of removing tri- and di- methyl marks from H3K4 (6). This subfamily is deregulated in several types of cancer and can modulate chemoresistance by numerous mechanisms including autophagy, epithelial-mesenchymal transition (EMT), stemness, metabolism and DNA repair (6,9). The role of KDM5s in the development of chemoresistance has been described in various types of cancer (10) KDM5A (11-14); KDM5B (15-21) and KDM5C (22-24).

The *KDM5D* gene (also known as *JARID1D* or *SMCY*) is located on the Y chromosome and it is the only male-specific KDM5. It is expressed in all male tissues, and carries out a role in spermatogenesis (25,26). KDM5D has been described as an important tumor-suppressor in castration-resistant prostate cancer and its low expression is associated with a worse prognosis (27). In prostate cancer, KDM5D regulates matrix metalloproteinase family genes associated with invasion, and loss of KDM5D with increased H3K4me3 levels in promoter regions of relevant genes increases invasiveness and metastatic ability (28,29). Moreover, in clear cell renal cell carcinoma (ccRCC), KDM5D is downregulated by loss of the Y chromosome, which contributes to the pathogenesis of ccRCC (30). In papillary renal cell carcinoma, KDM5D also facilitates demethylation of CDK4 and promotes proliferation of cancer cells (31). Chen *et al* (32) described the function of KDM5D in the development of CDDP tolerance in head and neck

Correspondence to: Professor Tomas Eckschlager, Department of Pediatric Hematology and Oncology, 2nd Faculty of Medicine, Charles University and Motol University Hospital, V Úvalu 84, 150 06 Prague 5, Czech Republic
E-mail: tomas.eckschlager@lfmotol.cuni.cz

Key words: neuroblastoma, KDM5D, chemoresistance, cisplatin, cullin 4A

squamous cell carcinoma (33). Decreased KDM5D expression was also observed in gastric, colorectal and hepatocellular carcinomas (34-36). Moreover, in an analysis of the Cancer Genome Atlas database, Duan *et al* (37) showed that KDM5D was notably downregulated in 24 different cancer types (such as breast, pancreatic and prostate cancer) compared with adjacent tissues. To the best of our knowledge, little is known about the importance of KDM5D in neuroblastoma. However, it has been reported that low KDM5D expression is associated with a worse prognosis in some tumors (38,39). We hypothesize that this is due to the decrease of cell junctions and therefore increase the ability to metastasize and due to the decrease of the presentation of antigens and therefore the immune response to the tumor (38,39).

CUL4A is a protein of the cullin family that acts as a scaffold for cullin RING ligase 4 complexes that promote ubiquitination of various substrates. It carries out an important role in DNA repair and replication, chromatin restructuring, cell cycle regulation, embryogenesis, hematopoiesis and spermatogenesis (40,41). There are a growing number of studies associating overexpression or amplification of *CUL4A* to increased growth, progression and metastasis in cancer (42-53). The *CUL4A* gene is located on 13q34, an area prone to amplification in some types of cancer (45-53). Shen *et al* (34) demonstrated that KDM5D carries out an important role in the induction of EMT of gastric cancer cells through demethylation in the promoter of *CUL4A* in male patients. In addition, another study suggests a relationship between the *CUL4A* gene and the sensitivity of colorectal cancer cells to CDDP (53).

Neuroblastoma is a malignancy of the sympathetic nervous system and is the most common malignant extracranial tumor of childhood. It is characterized by high degree of heterogeneity, which may account for the wide range of clinical presentations and variable response to treatment (54). The combination of clinical and genetic factors allows stratification of patients into very low, low, intermediate and high-risk groups (55). High-risk neuroblastoma is characterized by the development of acquired chemoresistance (56). To the best of our knowledge, there is currently little information regarding the role of KDM5D in neuroblastoma and the contribution of KDM5D to CDDP-chemoresistance.

The present study aims to investigate the importance of KDM5D expression for the proliferation of neuroblastoma cells and their chemoresistance to CDDP. On the basis of the aforementioned studies that demonstrated an association between KDM5D and CUL4A and their contribution to chemoresistance to CDDP, the present study investigated whether changes of CUL4A expression could be mediated by KDM5D in neuroblastoma cell lines.

Materials and methods

Cell culture and chemicals. Human high-risk neuroblastoma cell lines UKF-NB-3 and the derived CDDP-resistant line UKF-NB-3^{CDDP} were provided by Prof. Jindrich Cinatl, Goethe University, Frankfurt am Main, Germany. IMR-32 was purchased from MillporeSigma and SK-N-F1 by American Type Culture Collection. The CDDP-chemoresistant cell lines IMR-32^{CDDP} and SK-N-F1^{CDDP} were derived in our laboratory from their chemosensitive parental cell lines (IMR-32 and SK-N-F1) after long-term cultivation with increasing CDDP (Sandoz Group AG) concentration (57,58). All tested cell lines were of male origin. Cells were cultured at 37˚C and 5% CO_2 in Iscove's Modified Dulbecco's Medium (IMDM) supplemented with 10% (v/v) fetal bovine serum (both Thermo Fisher Scientific, Inc.). KDOAM-25 citrate (400 nM; HY-102047B; MedChemExpress) was used to inhibit KDM5s, where it was added to cells and incubated for 48 h at 37˚C.

KDM5 inhibition using KDOAM-25. For the inhibition of KDM5 demethylases, cells were treated with KDOAM-25 citrate for 24-48 h at 37˚C and 5% CO_2 (cat. no. HY-102047B; MedChemExpress) at a final concentration of 400 nM. This concentration was selected based on preliminary optimization experiments demonstrating efficient reduction of H3K4 trimethylation without affecting cell viability (data not shown). For supplementary validation experiments, KDOAM-25 was added 24 h before CDDP treatment, whereas for all main experiments presented in the manuscript, KDOAM-25 was added 48 h before CDDP administration and maintained throughout the treatment period.

Cell proliferation assay. To determine cell proliferation, cells were placed in 24-well plates ($1x10^5$ cells per well) or 96-well plates ($1x10^4$ cells per well) and seeded for 24 h at 37˚C.and then cells were treated with CDDP at a final concentration of 0.6-300 μM for 48 h at 37˚C. Cells were then incubated with PrestoBlue® Cell Viability Reagent (Thermo Fisher Scientific, Inc.) according to the manufacturer's protocol. Fluorescence was measured at an excitation wavelength of 560 nm and an emission wavelength of 590 nm using the SpectraMax® i3x Multi-Mode Microplate Reader (Molecular Devices, LLC). Each sample was analyzed in triplicate. The optical density of the medium was read as background, and the value of the optical density of the control cells was taken as 100%. IC_{50} values were calculated using SOFTmax® Pro 7.2 GxP software (Agilent Technologies, Inc.).

Transfection. On-Targetplus small interfering (si)RNA (Revvity Discovery Limited), a smart pool of three siRNAs [12.5 or 25 nM; cat. no. L-007948-00-0005; National Center for Biotechnology Information (NCBI) accession nos. NM_001146705.2, NM_001146706.2 and NM_004653.5] was used for silencing of KDM5D and On-Targetplus Non-Targeting control siRNA (12.5 or 25 nM; cat. no. D-001320-01-20), a smart pool of four siRNAs, was used as a negative control (Revvity Discovery Limited). For initial validation experiments, siRNA was tested at 12.5 and 25 nM. Based on these results, a final concentration of 25 nM was used for all subsequent functional experiments. siRNAs were transfected with Dharmafect transfection reagent (cat. no. T-2001-03; Revvity Discovery Limited) for 48 h according to the manufacturer's protocol. Following 48 h of incubation at 37˚C, cells were harvested and used for further analysis.

To ectopically express KDM5D, UKF-NB-3^{CDDP} cells were transfected for 48 h with the GenEZ™ ORF clone plasmid KDM5D pCMV-3Tag1a (OHu18895C; Genscript) designed for transcript variant 1 of KDM5D (8 and 16 ng/μl; NCBI accession number NM_001146705.1; GenScript Biotech Corporation) and pCMV6-AC-GFP, mammalian vector with

C-terminal tGFP tag (20 nM; OriGene Technologies, Inc.) was used as a negative control. For initial validation experiments, siRNA was tested at 8 and 16 ng/μl. Based on these results, a final concentration of 16 ng/μl was used for all subsequent functional experiments. The KDM5D ORF clone plasmid or control pCMV6-AC-GFP was transfected using Dharmafect transfection reagent (T-2001-03; Revvity Discovery Limited). The transfected cells were selected by Gibco geneticin™ Selective Antibiotic (cat. no. G418 Sulfate; 50 mg/ml) (Thermo Fisher Scientific, Inc.) in a final concentration 400 μg/ml for 72 h at 37˚C. Overexpression efficiency was determined by reverse transcription-quantitative polymerase chain reaction (RT-qPCR) and flow cytometry respectively.

The exact siRNA/shRNA sequences used in the present study are proprietary to Revvity Discovery Limited and are not publicly available. They can be obtained for manufacturer upon reasonable request (www.dharmacon.com).

RT-qPCR. mRNA from all NBL cell lines was isolated using the PureLink™ RNA Mini Kit (Thermo Fisher Scientific, Inc.) according to the manufacturer's protocol. The quality of the extracted mRNA was measured using the NanoDrop One spectrophotometer (260/280 nm ratio) (Thermo Fisher Scientific, Inc.). Complementary DNA was synthesized from 1.0 μg of mRNA using the Generi Biotech Reverse Transcription Kit according to the manufacturer's instructions (GENERI BIOTECH). RT-qPCR was performed using the gb Easy PCR Master Mix (cat. no. 3006; GENERI BIOTECH) according to the manufacturer's instructions, with custom primers (Generi custom oligo synthesis) and hydrolysis probes. The RT-qPCR assays are identified by Generi Biotech IDs. These assays can be ordered at ID (ID: 'hKDM5B_Q1' and 'hKDM5D_Q1') from GENERI BIOTECH. Expression levels of target genes and the internal control POLR2A (ID, hPOLR2A 'hPOLR2A_Q1'), which is homogeneously and uniformly expressed in neuroblastoma cell lines (59), were analyzed by RT-qPCR on a QuantStudio 3 Real-Time PCR System (Thermo Fisher Scientific, Inc.). Each sample was analyzed in triplicate. The thermocycling conditions were: 95˚C 3 min, 50 cycles of 95˚C for 10 sec, 60˚C 20 sec. The relative differences in gene expression were expressed as fold change and were obtained with the $2^{-\Delta\Delta Cq}$ method (Relative Expression Software Tool REST 2009 software, v2.0.11; QIAGEN) (60). The exact primer sequences used in the present study are proprietary to GENERI BIOTECH and are not publicly available. They can be obtained for manufacturer upon reasonable request (www.generi-biotech.com).

Cell cycle analysis. Cell cycle analysis was carried out using FxCycle™ Violet Ready Flow™ reagent (Thermo Fisher Scientific, Inc.). After treatment with CDDP and/or transfection, harvested neuroblastoma cells with 0.25% trypsin (Thermo Fisher Scientific, Inc.) were pelleted by centrifugation (300 x g) for 3 min at room temperature, resuspended in 100 μl of 3.6% paraformaldehyde (Biogen) and incubated at 20˚C for 15 min. After this incubation, the suspension was then centrifuged (300 x g) for 3 min at room temperature, and the pellet was washed twice with phosphate-buffered saline (PBS; Thermo Fisher Scientific, Inc.). Permeabilization was performed with 90% methanol (PENTA) for 1 h at -20˚C. Pellets were washed with PBS, resuspended in 500 μl of PBS and a drop of FxCycle™ Violet Ready Flow™ reagent was added. After 30 min of incubation at room temperature, cell cycle analysis was performed using a BD FACSCelesta (BD Biosciences) and data were analyzed using Flowlogic software, version 8 (Inivai Technologies).

Determination of protein levels and histone H3K4 methylation status by flow cytometry. After treatment with CDDP and/or transfection, harvested neuroblastoma cells (UKF-NB-3; UKF-NB-3^{CDDP}) were washed with cold PBS (Thermo Fisher Scientific, Inc.), trypsinized with 0.25% trypsin (Thermo Fisher Scientific, Inc.) and collected by centrifugation (300 x g) for 3 min at room temperature. Cell pellets were washed with PBS and fixed in 3.6% paraformaldehyde for 15 min at room temperature. The cell pellets were then washed with PBS and permeabilized with 90% methanol for 1 h at -20˚C. The pellets were then washed three times with 0.5% bovine serum albumin (BSA; Roth) in PBS. After washing, the cell pellets were blocked with 5% BSA in PBS for 1 hour at room temperature After blocking, the pellets were incubated with the primary antibody anti-JARID1D rabbit mAB at a dilution of 1:100 (cat. no. PA5-100844; Invitrogen, Thermo Fisher Scientific, Inc.), anti-JARID1B rabbit mAB at dilution of 1:400 (cat. no. 15327S; Cell Signaling Technology, Inc.), anti-trimethyl histone H3 (Lys4) rabbit (cat. no. 07-473; MilliporeSigma) at a dilution of 1:400, Cleaved-Caspase 3 (Asp175) Rabbit mAB at a dilution of 1:50 (cat. no. 9602S; Cell Signaling Technology, Inc.) or CUL4A Rabbit mAB at a dilution of 1:50 (cat. no 2699; Cell Signaling Technology, Inc.) for 1 h at laboratory temperature. Cell pellets were then washed with 0.5% BSA (Roth) and incubated in fluorochrome-conjugated secondary antibody Anti-Rabbit IgG (H+L) Alexa Fluor® 647 Conjugate (cat. no. A21245; Thermo Fisher Scientific, Inc.) diluted 1:500 and incubated for 30 min at room temperature in the dark. Cell pellets incubated with secondary antibody (1:500) only were used as a control. Washed and resuspended cells were measured using a BD FACSCelesta (BD Biosciences), and data were analyzed using Flowlogic software, version 8 (Inivai Technologies).

Cell migration monitoring. Real-time monitoring of cell migration of sensitive cells (UKF-NB-3) and their derived chemo-resistant cells (UKF-NB-3^{CDDP}) was carried out using the xCELLigence RTCA DP instrument (Agilent Technologies, Inc.) in a humidified incubator at 37˚C and 5% CO_2. For sensitive cells, KDM5D silencing (siKDM5D) and for CDDP-resistant UKF-NB-3^{CDDP} ORD cDNA transfection were performed. Cells were serum-starved for 2 h in IMDM without FBS at 37˚C and 5% CO_2. After the starvation period cells were trypsinized and seeded at a density of $1x10^4$ cells/well into upper chamber of the 16-well electronically integrated Boyden chamber for invasion/migration assays-CIM-plate 16 (RTCA, Agilent) containing starvation media. The wells of the lower chamber were loaded with IMDM with 10% FBS. As the cells migrated towards the chemoattractant across microelectronics sensors integrated at the bottom side of upper chamber, the impedance was measured every 30 min for 168 h at 37˚C. The measurements were recorded and analyzed using Real-Time Cell Analysis Software 1.2 (Agilent Technologies, Inc.).

Cell proliferation monitoring. Real-time monitoring of cell proliferation was carried out using the xCELLigence RTCA DP instrument (Agilent Technologies, Inc.) in a humidified incubator at 37˚C with 5% CO_2. Sensitive cells and their derived chemoresistant cells (UKF-NB-3, UKF-NB-3^{CDDP}, IMR-32, IMR-32^{CDDP}, SK-N-F1 or SK-N-F1^{CDDP}) were seeded at a concentration 8,000 cells per well in wells of 16-well E plates for impedance-based detection. For sensitive cells KDM5D silencing (siKDM5D) was carried out. After 48 h of transfection (siKDM5D), cells were seeded at a concentration 8,000 cells per well in wells of 16-well E plates for impedance-based detection. The cell index was monitored every 30 min for 96 h at 37˚C and data were recorded using the xCELLigence RTCA software Pro version 2.8 (Agilent Technologies Inc.) provided.

R2 genomics analysis and visualization platform. The R2 Genomics Platform (https://r2.amc.nl) is an open-access online genomic analysis and visualization platform that is publicly available to analyze and interpret clinical and genomic data. Several neuroblastoma datasets are available for survival analysis. The present study used three different datasets: i) Tumor neuroblastoma from Kocak (649; custom; ID: Agilent 44K microarray, Kocak dataset, Wolf normalization-ag44kcwolf;), which contains gene expression profiles from 649 patient-derived neuroblastoma tumors (https://hgserver1.amc.nl/cgi-bin/r2/main.cgi R2 internal identifier: ps_avgpres_gse45547geo649_ag44kcwolf) (61); ii) tumor neuroblastoma from SEQC (498; RPM; ID: SEQC/MAQC-III neuroblastoma dataset - seqcnb1), which contains expression data from gene expression microarrays for 498 patient-derived neuroblastoma tumors (https://hgserver1.amc.nl/cgi-bin/r2/main.cgi R2 internal identifier: ps_avgpres_gse62564geo498_seqcnb1) (62) and iii) tumor neuroblastoma from Oberthuer (251; user-defined; ID: Oberthuer neuroblastoma gene-expression dataset - amexp255), which consists of gene expression profiles from 251 patient-derived neuroblastoma tumors (https://hgserver1.amc.nl/cgi-bin/r2/main.cgi R2 internal identifier: ps_avgpres_nb251_amexp255) (63), (Table SI). To analyze the prognostic significance of the *KDM5D* and *CUL4A* genes Kaplan-Meier curves were generated comparing overall survival of patients with low and high expression of KDM5D or CUL4A using the integrated plotting function with default settings on R2: Genomics Analysis and Visualization Platform (Department of Oncogenomics, Amsterdam University Medical Centers (AMC), University of Amsterdam; accessed in 2024). Median expression cutoff mode and Bon-Ferroni correction for multiple testing was performed for all analyses. Statistical significance of survival differences was determined using the log-rank (Mantel-Cox) test.

Western blot analysis. Proteins were extracted from cultured neuroblastoma cells. Extraction of proteins was conducted using the ReadyPrep™ Protein Extraction Kit (Bio-Rad Laboratories, Inc.), with the addition of a complete protease inhibitor cocktail (Roche Applied Science). The concentration of proteins was subsequently measured using a BCA Protein Assay kit (Thermo Fisher Scientific Inc.). Samples (40 μg) were resolved on 4-20% precast gradient SDS-polyacrylamide gels (Mini-PROTEAN® TGX™, Bio-Rad Laboratories, Inc.), transferred onto PVDF membranes (Bio-Rad Laboratories, Inc.) and blotted on PVDF membranes (Bio-Rad Laboratories, Inc.). Membranes were blocked in 5% BSA in TBS containing 0.1% Tween-20 for 1 h at room temperature, followed by incubation with primary antibodies overnight at 4˚C. The following primary antibodies were used: KDM5D Rabbit pAb (cat. no. PA5-100844; Thermo Fisher Scientific, Inc.), was diluted to a concentration of 1:500, while CUL4A Rabbit pAb (cat. no. 2699S; Cell Signaling Technology Inc.) was diluted to 1:1,000. The PARP Rabbit pAb (cat. no. 9542S; Cell Signaling Technology Inc.) and the Caspase-3 Rabbit pAb (cat. no. 9622S; Cell Signaling Technology Inc.) were both diluted to 1:1,000. β-tubulin Mouse mAb (cat. no. 86298S, Cell Signaling Technology Inc.) was diluted to 1:1,000 and used as a loading control. Secondary antibodies, AlexaFluor 488 Mouse, Rabbit (cat. nos. A-11008 and A28175; Thermo Fisher Scientific Inc.) were diluted 1:2,000 and the incubation conditions were 1 h at room temperature. The membranes were then subjected to visualization via the ChemiDoc MP imaging system (Bio-Rad Laboratories, Inc.). The analysis was conducted utilizing ImageJ 1.52a software (National Institutes of Health).

For the verification of sustained KDM5D silencing, UKF-NB-3 cells were transfected with ON-TARGETplus KDM5D siRNA as described above and lysed at multiple time points up to 7 days after transfection. KDM5D protein levels were analyzed by western blotting using the KDM5D antibody and β-tubulin as a loading control.

Statistical analysis. All experiments were repeated independently at least three times, and data are expressed as mean ± standard error of the mean. ANOVA with post hoc Tukey honestly significant difference was used to compare different groups. One-way ANOVA with Tukey's post hoc test was used when a single independent variable (such as treatment, transfection or time) was analyzed. Two-way ANOVA with Tukey's post hoc test was applied when two independent variables (such as cell line and treatment) were analyzed simultaneously. Differences were considered statistically significant when. The exact statistical tests used for each analysis are indicated in the respective figure legends.

Results

Loss of KDM5D expression in CDDP resistant neuroblastoma cell line. Chemotherapy is one of the main treatment modalities for high-risk neuroblastoma, and CDDP is part of the majority of treatment protocols. The occurrence of chemoresistance is a considerable negative sign and contributes fundamentally to treatment failure. In this context, cell lines with intrinsic induced resistance to CDDP were analyzed. The IC_{50} of the CDDP-resistant cell lines (UKF-NB-3^{CDDP}, IMR-32^{CDDP} and SK-N-F1^{CDDP}) was significantly higher compared with the drug-sensitive parental lines UKF-NB-3, IMR-32 and SK-N-F1 (Figs. 1A and S1). In this group of cell lines, the mRNA and protein levels of KDM5D were examined in relation to CDDP resistance and CDDP treatment. The RT-qPCR results showed a loss of KDM5D expression in all CDDP-resistant cell lines. In addition, CDDP treatment decreased the expression of KDM5D in sensitive cells and this decrease was dependent on the duration of incubation with CDDP. The present study

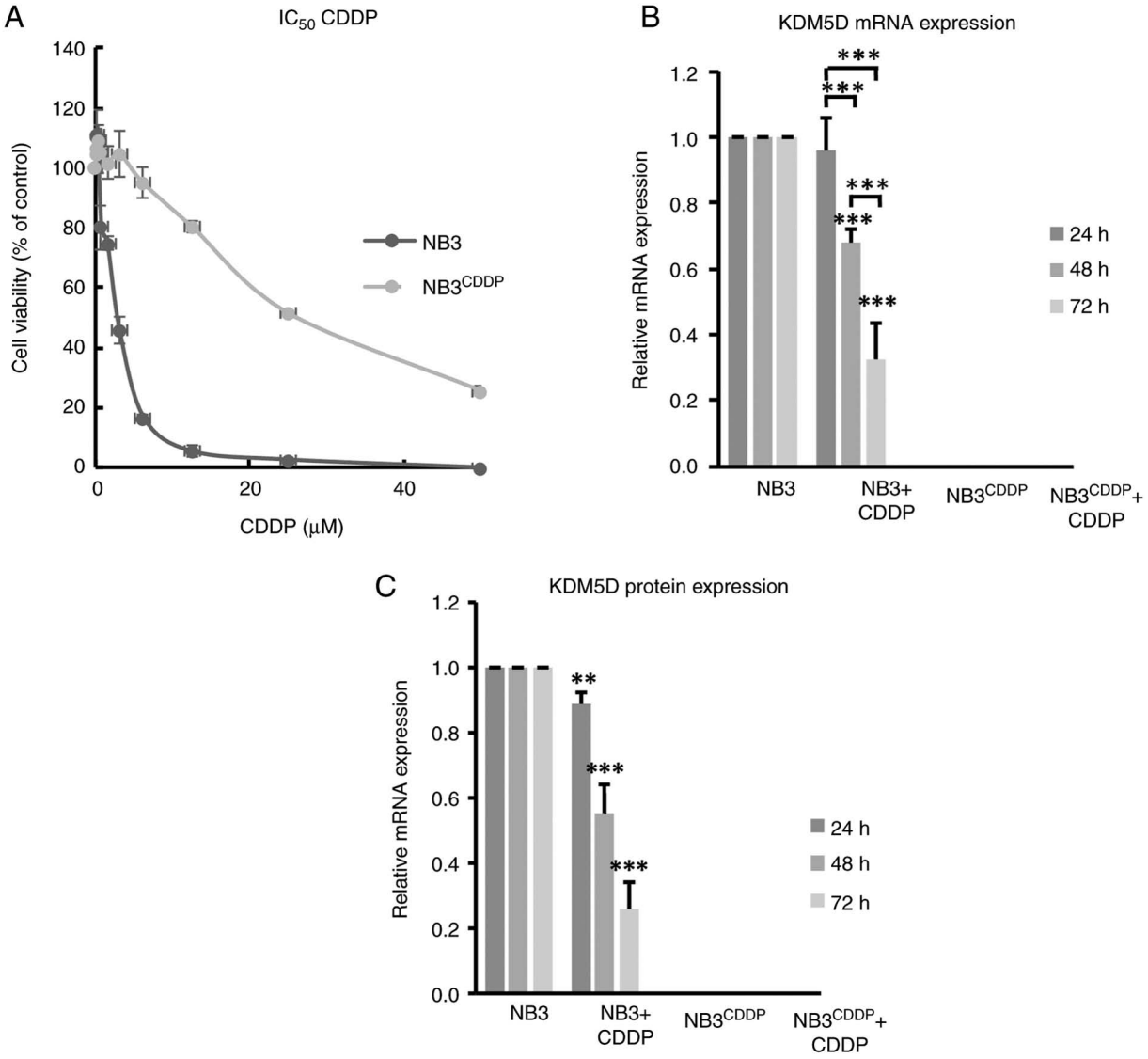

Figure 1. Loss of KDM5D expression in CDDP-resistant neuroblastoma cell line UKF-NB-3C^{CDDP}. PrestoBlue assay results showing cytotoxicity of CDDP after 72 h. (A) UKF-NB-3 has an IC_{50} of 13.33±0.97 μM and CDDP-resistant UKF-NB-3^{CDDP} has an IC_{50} of 32.39±0.96 μM. (B) KDM5D mRNA expression was lost in CDDP-resistant UKF-NB-3^{CDDP}. Treatment with 20 μM CDDP for 72 h significantly decreased KDM5D levels in UKF-NB-3. The mRNA expression was detected by reverse transcription-quantitative PCR. (C) KDM5D protein expression was detected by flow cytometry in UKF-NB-3 and CDDP-resistant UKF-NB-3^{CDDP} cell lines and showed the same pattern of expression as mRNA levels. Data are shown as mean ± standard deviation from three independent experiments. Statistical significance was determined using one-way ANOVA with Tukey's post hoc test. **P<0.01; ***P<0.001 (ANOVA with Tukey's post hoc). NB3, UKF-NB-3; NB3 CDDP, CDDP-resistant cell line UKF-NB-3^{CDDP}.

observed that no expression was present in drug-resistant cell lines even after treatment with CDDP (Figs. 1B and S1). The same results were observed at the protein level, as determined by means of flow cytometry (Figs. 1C and S1-S7). For further experiments, UKF-NB-3 and UKF-NB-3^{CDDP} cell lines were selected, as they were used previously to conduct a study with this cell line on the importance of KDM5B for CDDP-resistance (18).

KDM5D expression decreases histone H3K4 trimethylation in neuroblastoma cells. H3K4me3 is frequently associated with transcriptional activation of neighboring genes and therefore could activate oncogenes (64,65). We observed the change in trimethylation of H3K4 after CDDP treatment, silencing or overexpression of KDM5D in neuroblastoma cell lines (Fig. S8). To demonstrate the importance of KDM5D for methylation, the present study monitored H3K4 trimethylation after KDM5D silencing and overexpression. siRNA against *KDM5D* in the cell line UKF-NB-3 decreased expression levels of KDM5D mRNA (measured by RT-PqCR; Fig. 2A) and protein (measured by flow cytometry; Figs. 2B and S9) compared with non-coding siRNA-transfected control cells. Treatment of UKF-NB-3 with CDDP reduced KDM5D expression in controls, but did not further reduce expression in siRNA-transfected cells (Figs. 2C, D and S10). In addition, trimethylation of histone H3K4 was significantly increased in the KDM5D knockdown cells compared with the UKF-NB-3 control cells as shown by flow cytometry results, whereas the treatment with CDDP increased trimethylation only in the transfected cells, but not in control (Figs. 2E, F and S11).

The CDDP-resistant cell line UKF-NB-3^{CDDP}, which does not express KDM5D, was transfected with the KDM5D ORF

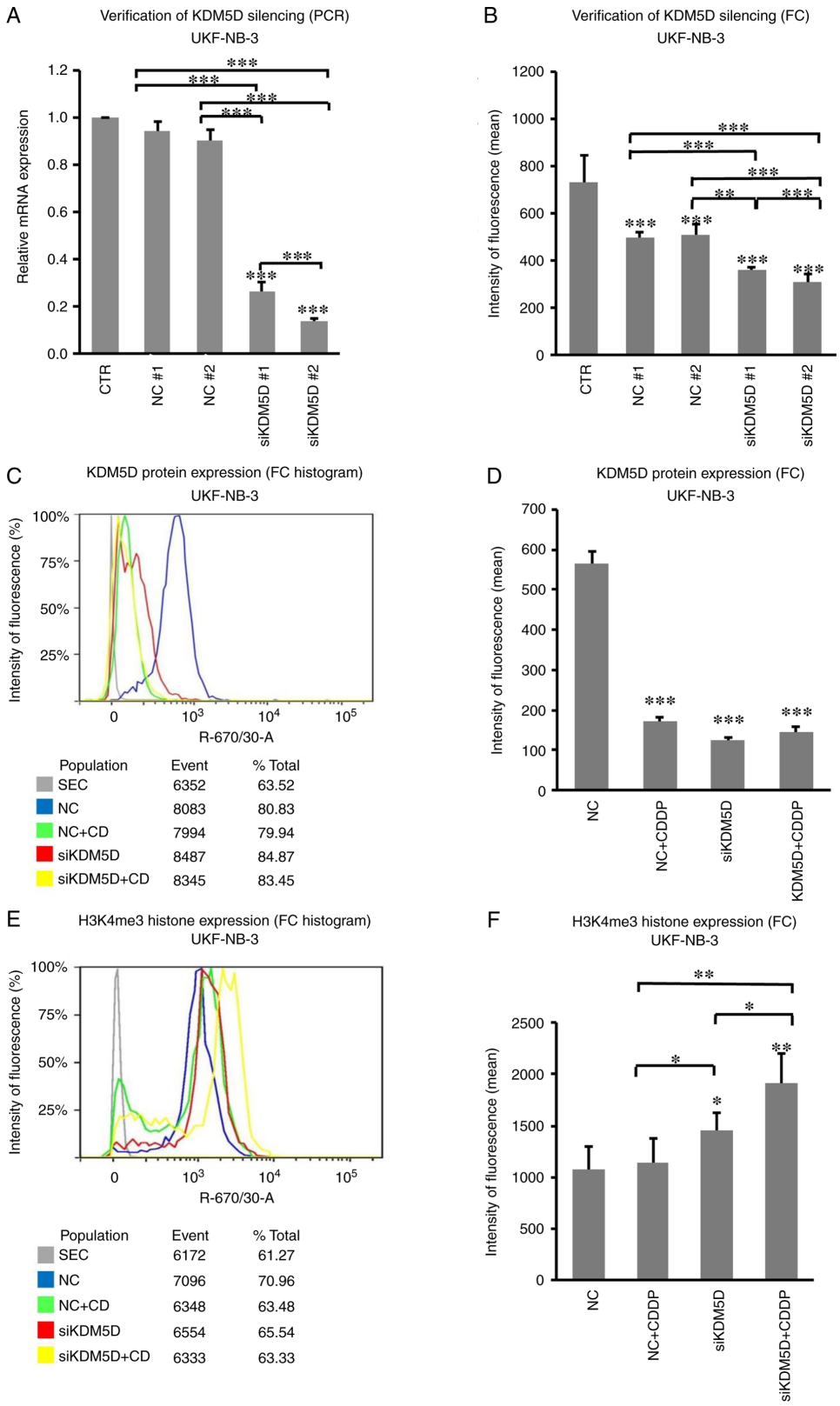

Figure 2. KDM5D knockdown affects histone H3K4 trimethylation in CDDP-sensitive neuroblastoma cell line UKF-NB-3. (A) Reverse transcription-quantitative PCR showed decreased expression of KDM5D mRNA in UKF-NB-3 cell line transfected with siKDM5D #1 (12.5 nM) or siKDM5D #2 (25 nM) compared to control NC #1 (12.5 nM) or NC #2 (25 nM) (P<0.001). (B) Reduced expression of KDM5D protein after siKDM5D transfection (48 h) was detected by flow cytometry (P<0.001). (C) Flow cytometry histogram showed decreased expression of KDM5D protein after siKDM5D transfection (48 h) and treatment with CDDP (48 h). (D) Flow cytometry showed decreased expression of KDM5D protein in control after treatment with CDDP in UKF-NB-3 (P<0.001) but did not further decrease the expression of KDM5D in transfected cells. (E) Flow cytometry histogram showed increased expression levels of histone H3K4 trimethylation after siKDM5D transfection (48 h). (F) Silencing of KDM5D increased the level of histone H3K4me3 trimethylation (P<0.01) and treatment with CDDP in UKF-NB-3 did not increase the level of H3K4me3 in control but further increased the level of histone H3K4me3 trimethylation in transfected cells (P<0.001). Data are shown as mean ± standard deviation from three independent experiments. Statistical significance was determined using one-way ANOVA with Tukey's post hoc test. *P<0.05; **P<0.01; ***P<0.001. CTR, control; si, short interfering RNA; SEC, control with only the secondary antibody; NC, control cells with non-coding RNA; siKDM5D, control cells transfected with siKDM5D; FC, flow cytometry.

clone plasmid pCMV-3Tag1 carrying the *KDM5D* gene for 48 h, resulting in overexpression of KDM5D at the protein level compared with cells transfected with the control plasmid (Figs. 3A and S12). In addition, treatment with CDDP decreased the expression of KDM5D in transfected cells (Figs. 3B, C and S13). Trimethylation of histone H3K4 was significantly decreased in cells transfected with *KDM5D* compared with control, while treatment with CDDP increased H3K4 trimethylation in both control and transfected cells (Figs. 3D, E and S14).

KDM5D expression increases the cell sensitivity to CDDP. To determine the effect of KDM5D expression on sensitivity to CDDP in neuroblastoma, the percentage of viable cells following treatment with CDDP at varying concentrations and time intervals was monitored. *KDM5D* knockdown did not affect the viability of cells in UKF-NB-3 after 24 h of transfection (Fig. S15) or after 48 h of transfection (Fig. 4A). The viability of KDM5D knockdown UKF-NB-3 cells decreased after incubation with CDDP depending on incubation time and concentration, but the decrease in viability of NC transfected cells after treatment with CDDP was more substantial (Figs. 4A and S16).

To compare the effect of inhibition of KDM5s demethylases on the viability and sensitivity of UKF-NB-3 and UKF-NB3^{CDDP} cells to CDDP, KDOAM-25 citrate was used as an inhibitor of the KDM5 demethylases subfamily (66), and therefore a concentration that effectively reduced H3K4 trimethylation without influencing cell survival (400 nM) was selected (data not shown). Inhibition of KDM5 by KDOAM-25 protected both sensitive (UKF-NB-3) and resistant (UKF-NB-3^{CDDP}) cells from the effects of CDDP (Fig. S16).

Overexpression of *KDM5D* did not alter cell viability in UKF-NB-3^{CDDP} after 24 h, even after incubation with CDDP (Fig. S17). However, after 48 h of incubation with CDDP, cell viability decreased with increasing CDDP concentration compared with mock-transfected controls, whose viability did not change after treatment with CDDP (Fig. 4B).

The decreased sensitivity to CDDP after incubation with the inhibitor was consistent with the downregulation of KDM5D by siRNA, and conversely, the increase in sensitivity to CDDP in the resistant line with induced KDM5D expression suggests the importance of KDM5D in the anticancer efficacy of CDDP.

Expression of KDM5D increases CDDP induced apoptosis in neuroblastoma cells. To determine whether overexpression of *KDM5D* in resistant cells and CDDP treatment induces apoptosis, activated caspase-3 and cleavage of PARP was examined to determine the relationship between the expression of KDM5D and CUL4A. Control cells had increased levels of activated caspase-3 after treatment with CDDP. Silencing of *KDM5D* in the sensitive cell line UKF-NB-3 did not change the amount of activated caspase-3 compared with control cells. Treatment with CDDP increased activated caspase-3, but the level of cleaved caspase-3 was significantly lower in cells with *KDM5D* knockdown compared with controls after CDDP treatment (Figs. 5A, S18 and S19). The KDM5 pan-inhibitor KDOAM-25 citrate had a similar effect as *KDM5D* silencing (Figs. S20-22). Overexpression of KDM5D resulted in an increase in activated caspase-3 level after treatment with CDDP in contrast with control cells (Figs. 5B and S23). Taken together, KDM5D is involved in the sensitivity to CDDP induced apoptosis in neuroblastoma cells.

KDM5D expression decreased S-phase, cell proliferation and migration. Because inhibition of KDM5D protects cells from the effect of CDDP (Figs. 4A, 5A, S15 and S16) and artificial expression, on the contrary, increases the effect of this cytostatic agent (Figs. 4B, 5B and S17), the present study focused on the significance of KDM5D for cell cycle and proliferation. In the sensitive cells, silencing of *KDM5D* resulted in an increase of cells in S phase and a decrease in G2/M phase compared with the control (Figs. 6A, S24 and C). Transfection of the plasmid with *KDM5D* in the cell line UKF-NB-3^{CDDP} decreased the percentage of cells in S phase and increased G0/G1 phase compared with control (Figs. 6B, S25A and E). Treatment with CDDP resulted in cell cycle arrest at checkpoint G0/G1 and G2/M in the sensitive cell line, and therefore the cell cycle was not evaluable (Fig. S24B, D, F).

The xCELLigence system was used to monitor cell migration (Figs. 6C and S26A) and proliferation (Figs. 6D and S26B-D) in real time, which showed that the CDDP-resistant UKF-NB-3^{CDDP} had a higher cell index of migration and proliferation compared with the CDDP-sensitive UKF-NB-3 with KDM5D expression. In addition, KDM5D knock down increased cell proliferation even in IMR-32 and SK-N-F1 lines (Fig. S26C-D). The silencing of KDM5D in UKF-NB-3 increased cell migration and proliferation, while KDM5D overexpression in UKF-NB-3^{CDDP} cells decreased migration and proliferation compared with controls. KDM5D silencing was verified over a period of 7 days using western blotting (Fig. S26E).

KDM5D plays a role in the development of chemoresistance to CDDP in neuroblastoma through regulation of the CUL4A gene. To assess the relationship between CUL4A and KDM5D (Fig. S18), its expression in CDDP-sensitive and resistant cells was examined. The CDDP-sensitive cell line UKF-NB-3 showed reduced expression of CUL4A protein compared with the CDDP-resistant UKF-NB-3^{CDDP}, and the expression of CUL4A increased after treatment with CDDP in the sensitive but not in the resistant cells (Figs. 7A, B S27 and S28). In addition, knockdown of *KDM5D* increased CUL4A expression Figs. 7B and S27). In UKF-NB-3^{CDDP} cells, overexpression of *KDM5D* decreased CUL4A expression compared with control, while CDDP treatment of cells with overexpressed *KDM5D* increased CUL4A expression levels. However, in the control, CDDP treatment did not alter CUL4A expression in resistant cells (Figs. 7C and S28). Inhibition of all KDM5s members by KDOAM-25 in sensitive cells increased level of CUL4A, compared with control but did not change CUL4A expression levels in chemoresistant cells that do not express KDM5D (Figs. S11 and S29-31).

Reduced expression of KDM5D is associated with poor overall survival. To investigate the role of *KDM5D* and *CUL4A* in neuroblastoma, patient data was screened from the R2 database: Genomics Analysis and Visualization Platform (http://r2.amc.nl). The association between *KDM5D* expression and overall survival was compared in male patients

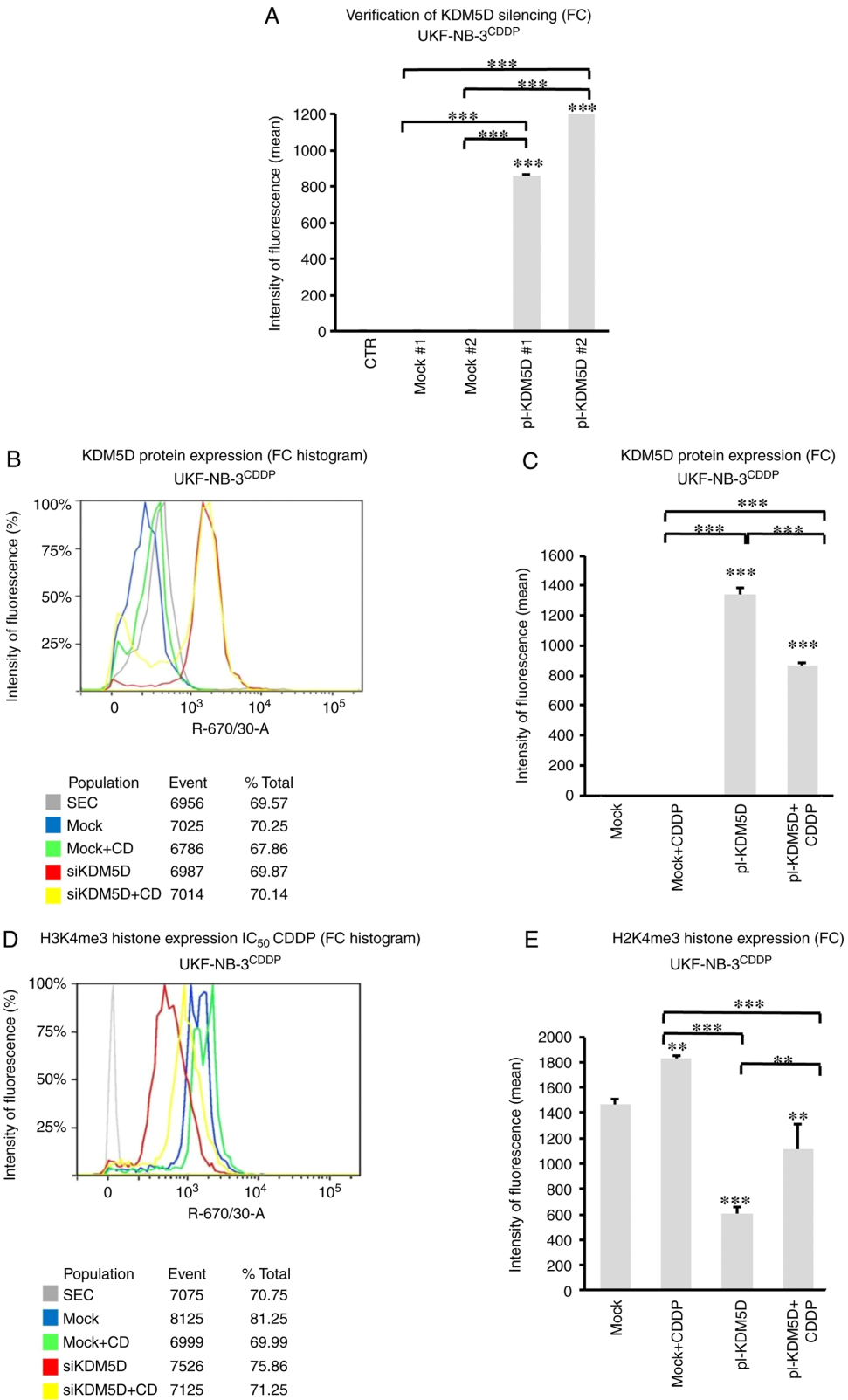

Figure 3. Aberrant expression of KDM5D affects histone H3K4 trimethylation in the CDDP-resistant neuroblastoma cell line UKF-NB-3^{CDDP}. (A) Flow cytometry showed increased levels of KDM5D protein in the UKF-NB-3^{CDDP} cell line transfected with the KDM5D ORF-clone plasmid pCMV-3Tag1, expressing the KDM5D gene (pl-KDM5D #, 8 ng/μl; or pl-KDM5D #2, 16 ng/μl) compared with control cells transfected with the control plasmid pCMV6-AC-GFP (mock #1, 8 ng/μl; or mock #2, 16 ng/μl), while control cells did not express KDM5D (P<0.001). (B) Flow cytometry histogram showed increased expression of KDM5D protein after KDM5D overexpression (48 h). (C) Flow cytometry proved increased protein level of KDM5D in KDM5D transfected UKF-NB-3^{CDDP} cells and showed that CDDP treatment in transfected cells decreased protein expression of KDM5D (P<0.001). (D) Flow cytometry histogram showed that histone H3K4 trimethylation decreased after KDM5D overexpression (48 h). (E) KDM5D overexpression decreased histone H3K4 trimethylation in UKF-NB-3^{CDDP} (P<0.001) but treatment with CDDP increased H3K4me3 trimethylation in transfected cells (P<0.05). Data are shown as mean ± standard deviation from three independent experiments. Statistical significance was determined using one-way (A) and two-way ANOVA (C, E) with Tukey's post hoc test **P<0.01; ***P<0.001. CTR, control; pl-ORF-clone plasmid; SEC, control with only the secondary antibody; Mock/NC, control cells with non-coding RNA; pl-KDM5D, control cells transfected with pl-KDM5D; FC, flow cytometry.

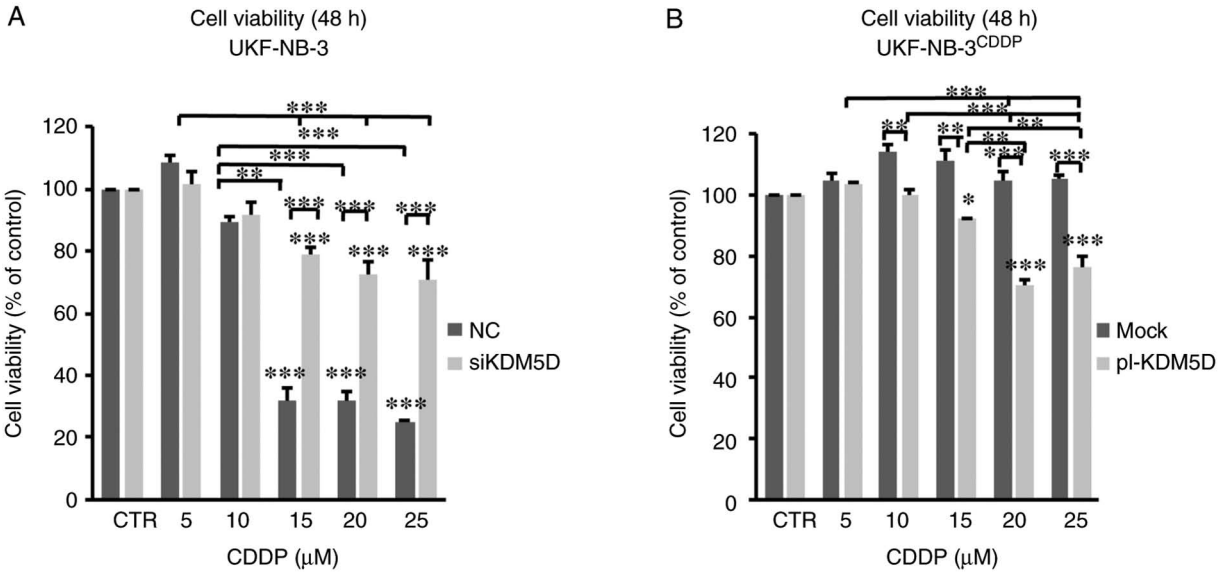

Figure 4. KDM5D expression affects cell sensitivity to CDDP in UKF-NB-3 and UKF-NB-3^{CDDP}. PrestoBlue assay results showed that incubation with CDDP (48 h) after (A) KDM5D silencing (48 h) in UKF-NB-3 caused reduced inhibition of cell viability induced by CDDP in silenced cells compared with NC after treatment with increasing concentrations of CDDP (P<0.001). (B) Overexpression of KDM5D in UKF-NB-3^{CDDP} made the cells more sensitive to CDDP compared with mock (P<0.5; P<0.001). Data are shown are mean ± standard deviation from three independent experiments. Statistical significance was determined using two-way ANOVA with Tukey's post hoc test. *P<0.05; **P<0.01; ***P<0.001 (ANOVA with Tukey's post hoc test). CTR, control; si, short interfering RNA; pl, ORF-clone plasmid.

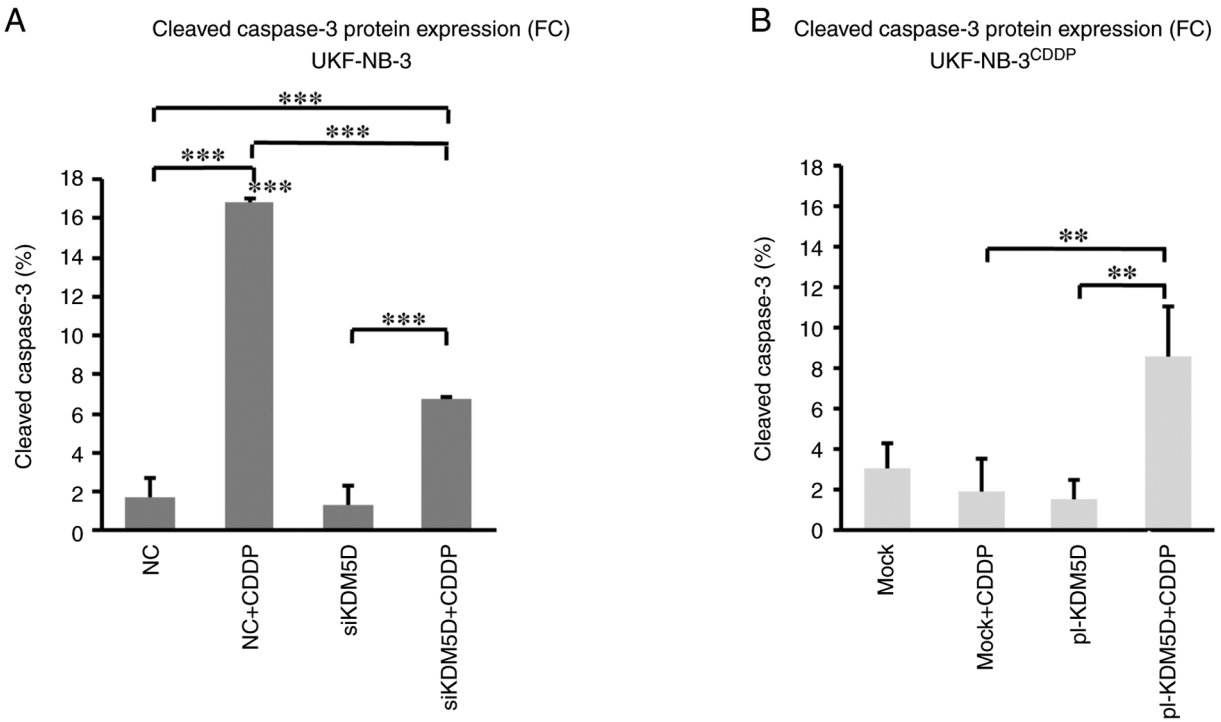

Figure 5. Expression of KDM5D increases CDDP induced apoptosis in neuroblastoma cells. (A) Cleaved caspase-3 in CDDP sensitive cell line UKF-NB-3 and (B) CDDP resistant cell line UKF-NB-3^{CDDP}. Sensitive cell line UKF-NB-3 had increased levels of activated caspase-3 after CDDP treatment (P<0.001), where silencing of KDM5D led to decreased levels compared with NC (P<0.001). In CDDP-resistant cell line UKF-NB-3^{CDDP}, CDDP treatment after transfection with plasmid with KDM5D gene, increased activated caspase-3 level (P<0.01) compared with mock. Data are shown as mean ± standard deviation from three independent experiments. Statistical significance was determined using two-way ANOVA with Tukey's post hoc test **P<0.01; ***P<0.001. si, short interfering RNA; pl, ORF-clone plasmid; Mock/NC, control cells with non-coding RNA; siKDM5D/pl-KDM5D, control cells transfected with siKDM5D/pl-KDM5D; FC, flow cytometry.

with two different neuroblastoma risk groups according to International Neuroblastoma Staging System (INSS) stages: non-high-risk (st1, st2, st3 and st4S) and high-risk (st4) (67). This analysis showed that low *KDM5D* expression was associated with poor survival rates in the group with st4 (Figs. 8B and S32). Analysis of three different datasets of patients with

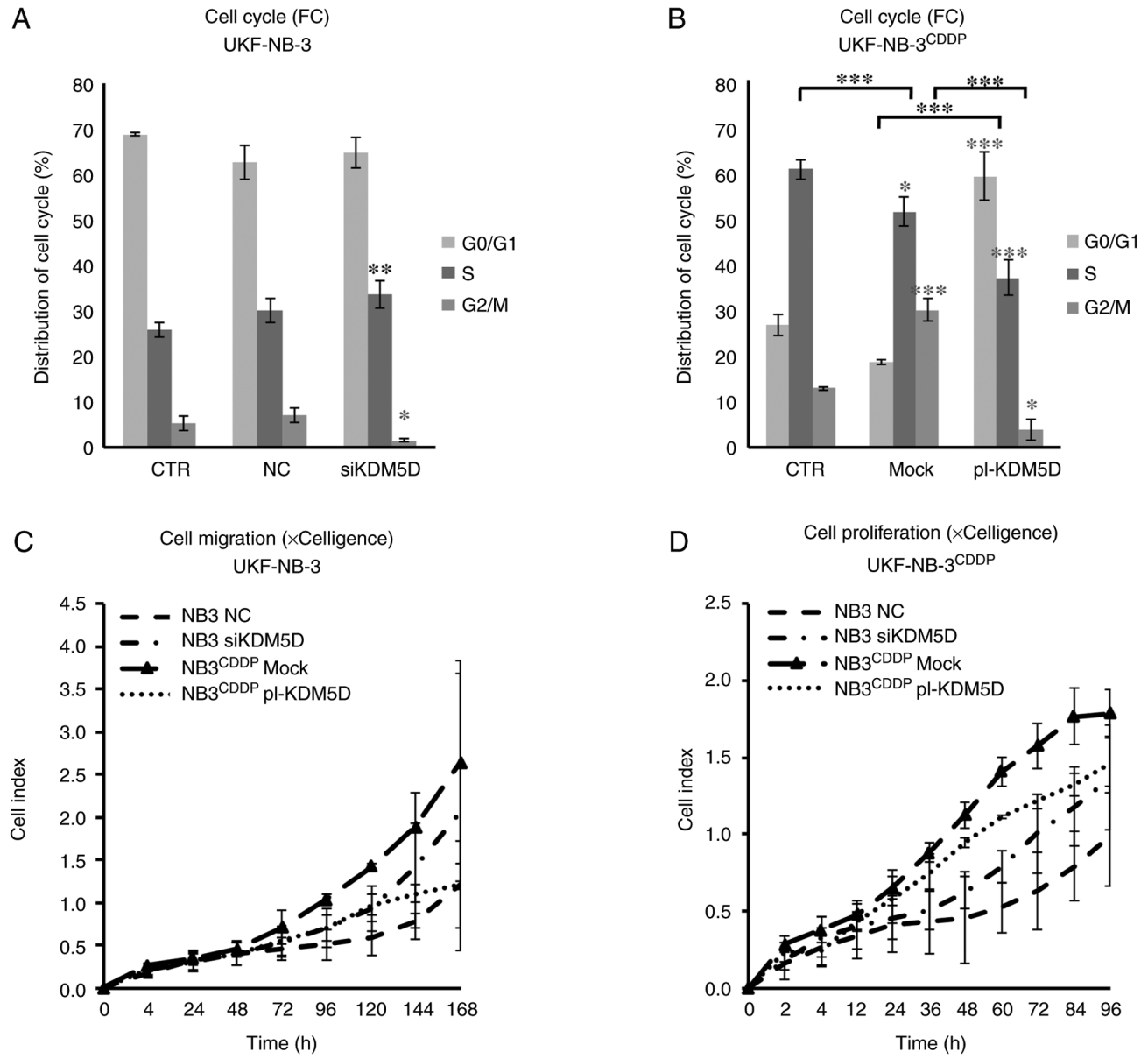

Figure 6. Flow cytometry analysis of cell cycle, proliferation and cell migration by xCELLigence in CDDP-sensitive cell line UKF-NB-3 and CDDP-resistant cell line UKF-NB-3^{CDDP}. (A) Silencing of KDM5D in sensitive cell line UKF-NB-3 led to increased S phase ($P<0.01$) and decreased G2/M phase ($P<0.05$) compared with control or cells with NC. (B) Transfection of plasmid with KDM5D in CDDP-resistant cell line UKF-NB-3^{CDDP} led to decreased S phase ($P<0.001$) and increased G0/G1 phase ($P<0.01$) compared with control or mock ($P<0.001$). (C) Monitoring of cell migration by xCELLigence after transfection of siKDM5D in UKF-NB-3 or ORF cDNA plasmid with KDM5D gene in UKF-NB-3^{CDDP}. (D) Monitoring of cell proliferation by xCELLigence after transfection of siKDM5D in UKF-NB-3 or ORF cDNA plasmid with KDM5D gene in UKF-NB-3^{CDDP}. Data are shown as mean ± standard deviation from three independent experiments. Statistical significance was determined using one-way ANOVA (A) and two-way ANOVA (B, C and D) with Tukey's post hoc test. $^{*}P<0.05$; $^{**}P<0.01$; $^{***}P<0.001$ (ANOVA with Tukey's post hoc test). CTR, control; NC, non-coding RNA; si, short interfering RNA; pl, ORF-clone plasmid; NB3, UKF-NB-3; FC, flow cytometry.

neuroblastoma from the R2 platform indicated a statistically significant correlation between *KDM5D* expression and higher survival rates in high-risk neuroblastoma patients. In the non-high-risk group, there was not a significant difference in all data sets (Figs. 8A and S32). These observations are consistent with our hypothesis that low KDM5D concentration in neuroblastoma has tumor-promoting effects and is associated with chemoresistance.

To uncover the relationship between the expression of *KDM5D* and *CUL4A*, the present study further analyzed the data from the aforementioned databases in R2: for an association between the expression of *CUL4A* and overall survival of neuroblastoma patients. Kaplan-Meier analysis in these datasets revealed that high relative expression of *CUL4A* is often associated with worse survival in two datasets of patients with stages 1, 2, 3 or 4S (Figs. 8D and S33); moreover, this association is significant in stage 4 (Figs. 8E and S32), however, this was not true in the Oberthuer dataset.

Discussion

It is well known that in cancer, aberrant epigenetic modifications, which include histone methylation, contribute to various stages of neoplastic development, including initiation, promotion,

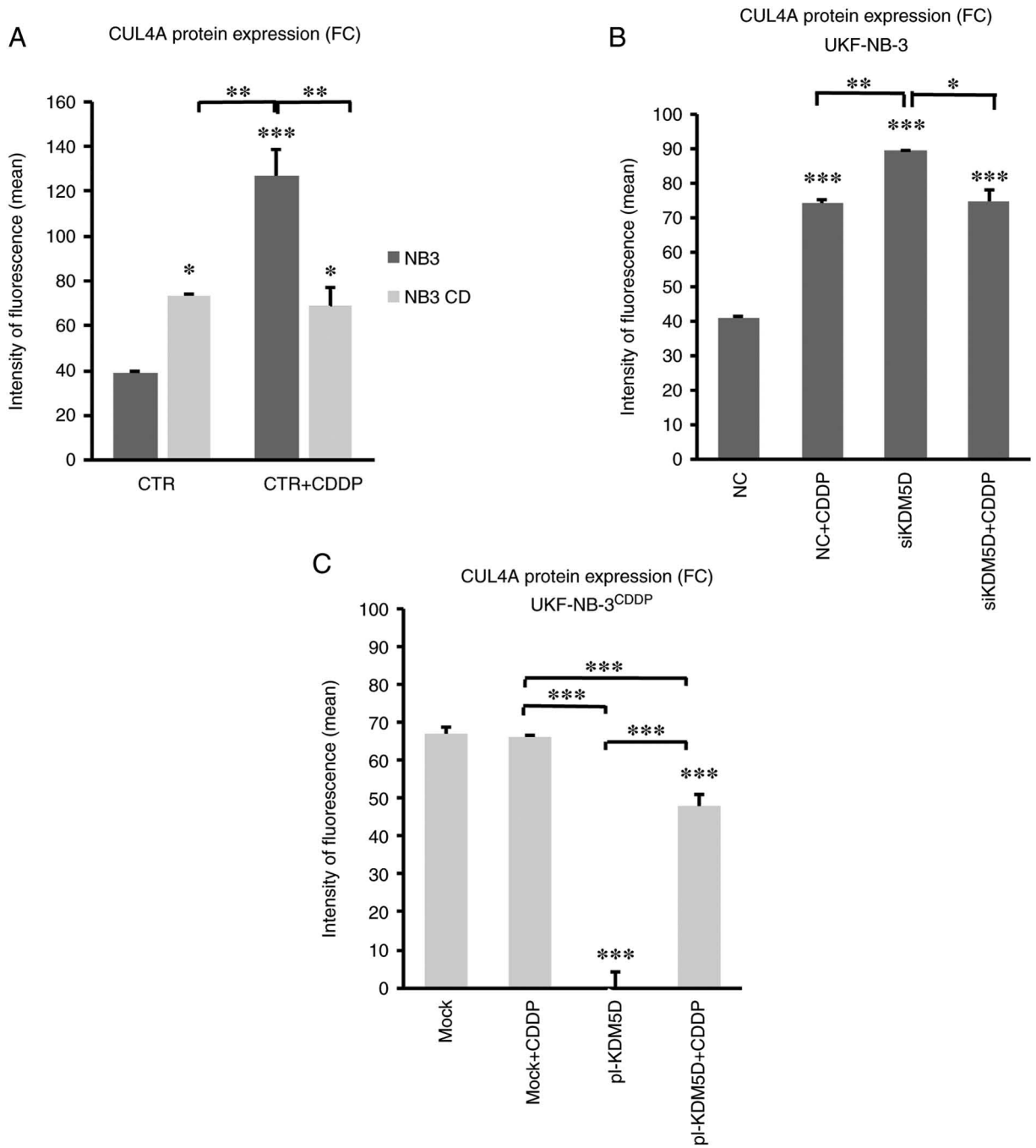

Figure 7. KDM5D and CDDP treatment affect expression of CUL4A in UKF-NB-3 and UKF-NB-3$^{CDDP.}$ Flow cytometry analysis in (A) UKF-NB-3 and UKF-NB-3^{CDDP}, where sensitive cell line UKF-NB-3 showed lower expression of CUL4A gene compared with the resistant cell line ($P<0.05$) and this expression increased in sensitive cells after CDDP treatment ($P<0.001$) compared with control. (B) Silencing of KDM5D increased of CUL4A level ($P<0.001$). (C) In the CDDP-resistant cell line UKF-NB-3^{CDDP}, KDM5D overexpression decreased CUL4A expression compared with mock and control plasmid ($P<0.001$). CDDP treatment of overexpressed cells with KDM5D increased the level of CUL4A ($P<0.001$), while in control cells CDDP treatment did not change the level of CUL4A. Data are shown as mean ± standard deviation from three independent experiments. Statistical significance was determined using two-way ANOVA with Tukey's post hoc test. $^{*}P<0.05$; $^{**}P<0.01$; $^{***}P<0.001$ (ANOVA with Tukey's post hoc test). CTR, control; NC, non-coding RNA; si, short interfering RNA; pl, ORF-clone plasmid; NB3, UKF-NB-3; Mock/NC, control cells; siKDM5D/pl-KDM5D, control cells transfected with siKDM5D/pl-KDM5D; FC, flow cytometry.

invasion, metastasis, EMT and chemoresistance (1-5). There is increasing evidence for the importance of histone lysine demethylase function, the dysregulation of which has been described in several types of cancer (8,9). Aberrant expression of KDM5D has been observed in a number of types of cancer (27-33). According to the results of analysis of publicly available genomics data, the present study found that low expression of KDM5D is associated with worse survival in male patients with stage 4 neuroblastoma. As drug resistance often develops in high-risk neuroblastoma (53,54), the present study investigated the role of KDM5D in the development of chemoresistance to CDDP, which is commonly used in therapy of the high-risk neuroblastoma (68).

The present study demonstrated that expression of KDM5D was lost in all tested CDDP-resistant neuroblastoma cell lines

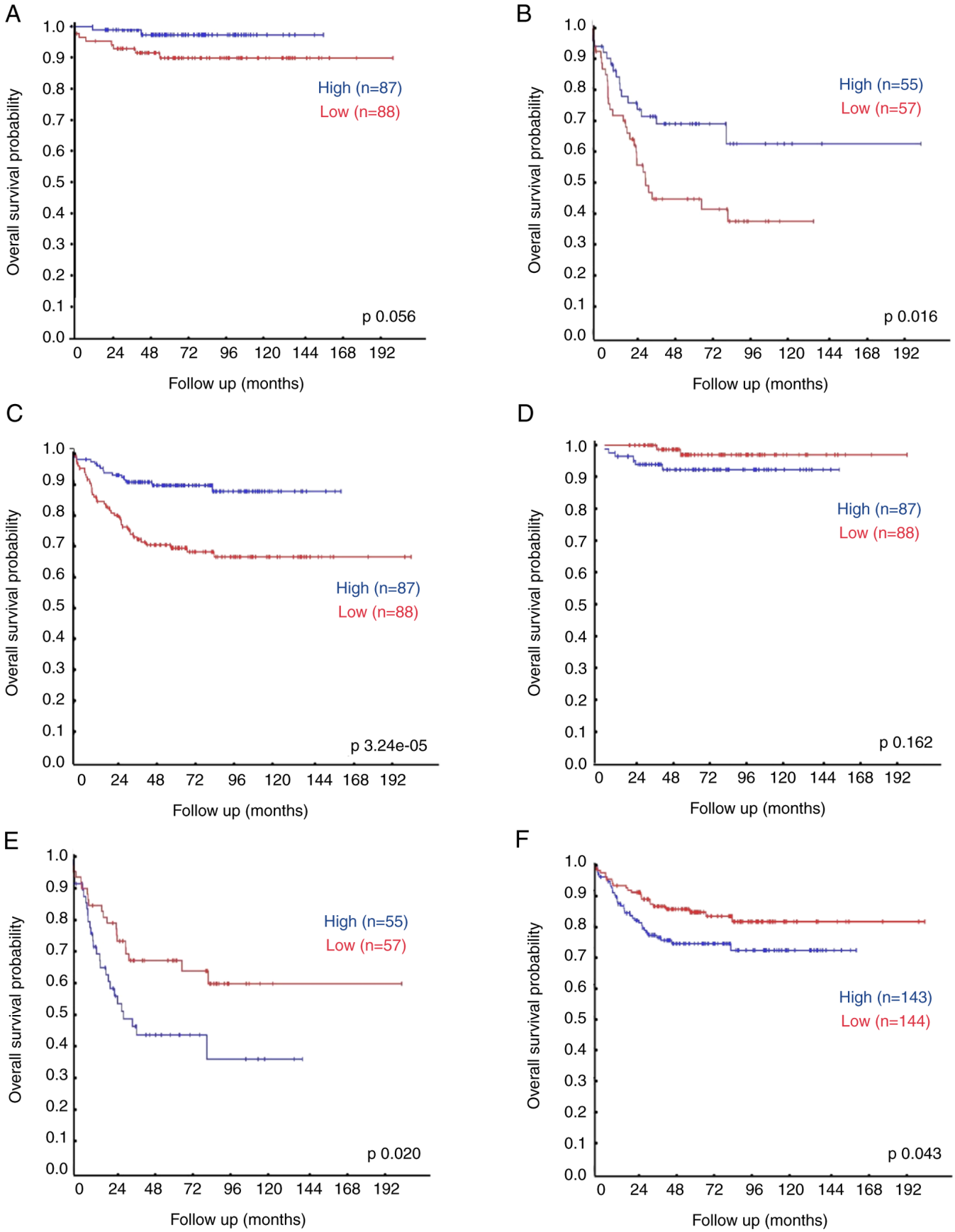

Figure 8. Kaplan-Meier curves analyzing KDM5D (A, B, C) and CUL4A (D, E, F) expression data and overall survival of patients in the SEQC neuroblastoma dataset (498; RPM; seqcnb1): (A) Male patients with stages 1, 2, 3 and 4S, KDM5AD expression. (B) Male patients with stage 4, KDM5D expression. (C) All male patients according to the International Neuroblastoma Staging System, KDM5D expression. (D) Male patients with stages 1, 2, 3 and 4S, CUL4A expression. (E) Male patients with stage 4, CUL4A expression. (F) All male patients according to the International Neuroblastoma Staging System, CUL4A expression. Statistical significance of survival differences was determined using the log-rank (Mantel-Cox) test. R2: Genomics Analysis and Visualization Platform revealed that low relative expression of KDM5D and high expression of CUL4A is associated with worse survival.

compared with sensitive parental cells. Silencing of *KDM5D* in the sensitive neuroblastoma cell lines resulted in increased trimethylation of H3K4, decreased sensitivity of cells to CDDP, inhibition of apoptosis induced by CDDP, increased proliferation and proportion of cells in S phase and acceleration of cell migration. To date, limited studies have been published describing the relationship between KDM5D and chemoresistance. Komura *et al* (27) found that KDM5D plays an important role as a tumor-suppressor in castration-resistant prostate cancer, where it activates the androgen receptor, and low KDM5D expression associates with docetaxel insensitivity, aggressiveness and worse prognosis. KDM5D, along with five other Y-linked genes, is reported to be downregulated in 12 major non-reproductive types of cancer, suggesting selection against their activity and their function as tumor-suppressors (69,70). Moreover, loss of the Y chromosome was described as being associated with shorter overall survival and resistance to radiotherapy and cisplatin-based chemotherapeutics in male neck squamous cell carcinoma (66,71). The present study also observed that the CDDP-resistant neuroblastoma cell line had increased expression of CUL4A compared with the sensitive parental cells and that KDM5D knockdown in the sensitive cells increased CUL4A.

The present study concludes that low expression of KDM5D is associated with worse survival in male patients with neuroblastoma, as shown by analysis of publicly available genomics data. Accordingly, the present study examined neuroblastoma cell lines with genotype XY and showed that all CDDP-resistant cell lines had KDM5D expression below the detection limit. Silencing of KDM5D results in increased trimethylation of histone H3K4 or *vice versa* overexpression decreased H3K4 trimethylation in CDDP-resistant cells. Our previous study demonstrated an increase in H3K4me3 after silencing of KDM5B (18), therefore all members of the KDM5 subfamily may potentially have an important function in regulating of H3K4 methylation.

Results of the present study demonstrate that KDM5D expression affects proliferation, migration and sensitivity of neuroblastoma cells to CDDP. Both the reduction of KDM5D expression in cells due to cytostatics and the more selective toxicity of cytostatics towards cells with increased expression of KDM5D and thus the selection of cells with lower expression can be applied. The concentration of CDDP (20 μM) used markedly reduced cell viability compared with controls after a 24 h incubation, and KDM5D expression values measured by RT-qPCR at this time interval were reduced insignificantly. From this, it is difficult to draw conclusions about which of the mechanisms applies.

Finally, the present study examined the expression of the gene *CUL4A*. Sensitive cell lines showed reduced expression of *CUL4A* compared with resistant ones. Moreover, this expression increased after silencing of KDM5D, CDDP or KDOAM-25 treatment in CDDP-sensitive but not in resistant cells, which do not express KDM5D. These findings suggest that CDDP and KDOAM-25 affect CUL4A expression *via* KDM5D. The relationship between the expression of KDM5D and CUL4A was described by Shen *et al* (34) in a study demonstrating that KDM5D regulates the methylation of H3K4 in the promoter of CUL4A and represses the expression of CUL4A. This study revealed that CUL4A expression plays an important role in metastasis and EMT of gastric cancer cells but to the best of our knowledge, there is no information regarding the importance of CUL4A in neuroblastoma.

Englinger *et al* (53) showed that loss of CUL4A expression leads to hypersensitivity to CDDP in colon cancer cells. Downregulation of *CUL4A* mediated a lack of nucleotide excision repair that caused trabedectin resistance and collateral CDDP hypersensitivity in colorectal carcinomas.

Overall, in CDDP-resistant neuroblastoma cell lines, there is a loss of KDM5D expression that leads to a more aggressive phenotype of neuroblastoma by promoting cell proliferation and migration, evading cell death, promoting S phase of the cell cycle and desensitizing susceptible cells to CDDP. The data of the present study may suggest that the change in expression is caused by demethylation of H3K4 in the *CUL4A* gene. The precise mechanisms by which KDM5D and CUL4A are involved in the development of chemoresistance remain to be elucidated. To the best of our knowledge, the relationship between KDM5D and CUL4A in neuroblastoma has not yet been studied. We hypothesize that KDM5D and/or CUL4A may be a useful biomarker for detection of chemoresistance in clinical practice and that inhibition of CUL4A may be a potential therapeutic approach in neuroblastoma after further preclinical and clinical studies.

Acknowledgements

Not applicable.

Funding

This research was funded by the Grant Agency of Charles University, Czech Republic (grant no. 822219) and by Ministry of Health of the Czech Republic (grant no. NW24-03-00101).

Availability of data and materials

The data generated in the present study may be requested from the corresponding author.

Authors' contributions

TE conceived and led the present study. NP performed sample preparation, RT-qPCR, flow cytometry, cell proliferation assay, siRNA and ORF cDNA transfection, cell proliferation monitoring, data analysis, and the statistical analysis, and wrote the manuscript. JH contributed to the acquisition of data by performing part of the flow cytometry experiments and assisting in data interpretation. MB contributed to the acquisition of data by preparing biological samples and performing part of the RT-qPCR experiments, and assisted in data interpretation. NP, TE, JH and MB confirm the authenticity of all the raw data. All authors have reviewed the manuscript and read and approved the final manuscript.

Ethics approval and consent to participate

Not applicable.

Patient consent for publication

Not applicable.

Competing interests

The authors declare that they have no competing interests.

References

1. Barski A, Cuddapah S, Cui K, Roh TY, Schones DE, Wang Z, Wei G, Chepelev I and Zhao K: High-resolution profiling of histone methylations in the human genome. Cell 129: 823-837, 2007.
2. Mikkelsen TS, Ku M, Jaffe DB, Issac B, Lieberman E, Giannoukos G, Alvarez P, Brockman W, Kim TK, Koche RP, *et al*: Genome-wide maps of chromatin state in pluripotent and lineage-committed cells. Nature 448: 553-560, 2007.
3. Tsukada YI, Fang J, Erdjument-Bromage H, Warren ME, Borchers CH, Tempst P and Zhang Y: Histone demethylation by a family of JmjC domain-containing proteins. Nature 439: 811-816, 2006.
4. Shukla A, Chaurasia P and Bhaumik SR: Histone methylation and ubiquitination with their cross-talk and roles in gene expression and stability. Cell Mol Life Sci 66: 1419-1433, 2009.
5. Jambhekar A, Dhall A and Shi Y: Roles and regulation of histone methylation in animal development. Nat Rev Mol Cell Biol 20: 625-641, 2019.
6. Plch J, Hrabeta J and Eckschlager T: KDM5 demethylases and their role in cancer cell chemoresistance. Int J Cancer 144: 221-231, 2019.
7. Ruthenburg AJ, Allis CD and Wysocka J: Methylation of lysine 4 on histone H3: Intricacy of writing and reading a single epigenetic mark. Mol Cell 25: 15-30, 2007.
8. Arifuzzaman S, Khatun MR and Khatun R: Emerging of lysine demethylases (KDMs): From pathophysiological insights to novel therapeutic opportunities. Biomed Pharmacother 129: 110392, 2020.
9. Sterling J, Menezes SV, Abbassi RH and Munoz L: Histone lysine demethylases and their functions in cancer. Int J Cancer 148: 2375-2388, 2021.
10. Wang N, Ma T and Yu B: Targeting epigenetic regulators to overcome drug resistance in cancers. Signal Transduct Target Ther 8: 69, 2023.
11. Wu H, Xu L and Hu X: KDM5A regulates the growth and gefitinib drug resistance against human lung adenocarcinoma cells. 3 Biotech 12: 97, 2022.
12. Banelli B, Carra E, Barbieri F, Würth R, Parodi F, Pattarozzi A, Carosio R, Forlani A, Allemanni G, Marubbi D, *et al*: The histone demethylase KDM5A is a key factor for the resistance to temozolomide in glioblastoma. Cell Cycle 14: 3418-3429, 2015.
13. Feng T, Wang Y, Lang Y and Zhang Y: KDM5A promotes proliferation and EMT in ovarian cancer and closely correlates with PTX resistance. Mol Med Rep 16: 3573-3580, 2017.
14. Hou J, Wu J, Dombkowski A, Zhang K, Holowatyj A, Boerner JL and Yang ZQ: Genomic amplification and a role in drug-resistance for the KDM5A histone demethylase in breast cancer. Am J Transl Res 4: 247-256, 2012.
15. Roesch A, Vultur A, Bogeski I, Wang H, Zimmermann KM, Speicher D, Körbel C, Laschke MW, Gimotty PA, Philipp SE, *et al*: Overcoming intrinsic multidrug resistance in melanoma by blocking the mitochondrial respiratory chain of slow-cycling JARID1B high cells. Cancer Cell 23: 811-825, 2013.
16. Xu W, Zhou B, Zhao X, Zhu L, Xu J, Jiang Z, Chen D, Wei Q, Han M, Feng L, *et al*: KDM5B demethylates H3K4 to recruit XRCC1 and promote chemoresistance. Int J Biol Sci 14: 1122-1132, 2018.
17. Liu J and Nie C: KDM5B regulates the PTEN/PI3K/Akt pathway to increase sorafenib-resistance in hepatocellular carcinoma. Anticancer Drugs 33: 840-849, 2022.
18. Belhajova M, Podhorska N, Vicha A and Eckschlager T: KDM5B expression in cisplatin resistant neuroblastoma cell lines. Oncol Lett 24: 365, 2022.
19. Kuo YT, Liu YL, Adebayo BO, Shih PH, Lee WH, Wang LS, Liao YF, Hsu WM, Yeh CT and Lin CM: JARID1B expression plays a critical role in chemoresistance and stem cell-like phenotype of neuroblastoma cells. PLoS One 10: e0125343, 2015.
20. Li L, Shou H, Wang Q and Liu S: Investigation of the potential theranostic role of KDM5B/miR-29c signaling axis in paclitaxel resistant endometrial carcinoma. Gene 694: 76-82, 2019.
21. Wang L, Mao Y, Du G, He C and Han S: Overexpression of JARID1B is associated with poor prognosis and chemotherapy resistance in epithelial ovarian cancer. Tumor Biol 36: 2465-2472, 2015.
22. Lin H, Yang G, Yu J, Wang J, Li Q, Guo S and Cao B: KDM5C inhibits multidrug resistance of colon cancer cell line by down-regulating ABCC1. Biomed Pharmacother 107: 1205-1209, 2018.
23. Hong Z, Wu G, Xiang ZD, Xu CD, Huang SS, Li C, Shi L and Wu DL: KDM5C is transcriptionally regulated by BRD4 and promotes castration-resistance prostate cancer cell proliferation by repressing PTEN. Biomed Pharmacother 114: 108793, 2019.
24. Outchkourov NS, Muiño JM, Kaufmann K, van IJcken WF, Groot Koerkamp MJ, van Leenen D, de Graaf P, Holstege FC, Grosveld FG and Timmers HT: Balancing of histone H3K4 methylation states by the Kdm5c/SMCX histone demethylase modulates promoter and enhancer function. Cell Rep 3: 1071-1079, 2013.
25. Agulnik AI, Longepied G, Ty MT, Bishop CE and Mitchell M0020: Mouse H-Y encoding Smcy gene and its X chromosomal homolog Smcx. Mamm Genome 10: 926-929, 1999.
26. Akimoto C, Kitagawa H, Matsumoto T and Kato S: Spermatogenesis-specific association of SMCY and MSH5. Genes Cells 13: 623-633, 2008.
27. Komura K, Jeong SH, Hinohara K, Qu F, Wang X, Hiraki M, Azuma H, Lee GS, Kantoff PW and Sweeney CJ: Resistance to docetaxel in prostate cancer is associated with androgen receptor activation and loss of KDM5D expression. Proc Natl Acad Sci USA 113: 6259-6264, 2016.
28. Jangravi Z, Tabar MS, Mirzaei M, Parsamatin P, Vakilian H, Alikhani M, Shabani M, Haynes PA, Goodchild AK, Gourabi H, *et al*: Two splice variants of Y chromosome-located lysine-specific Demethylase 5D have distinct function in prostate cancer cell line (DU-145). J Proteome Res 14: 3492-3502, 2015.
29. Li N, Dhar SS, Chen TY, Kan PY, Wei Y, Kim JH, Chan CH, Lin HK, Hung MC and Lee MG: JARID1D is a suppressor and prognostic marker of prostate cancer invasion and metastasis. Cancer Res 76: 831-843, 2016.
30. Arseneault M, Monlong J, Vasudev NS, Laskar RS, Safisamghabadi M, Harnden P, Egevad L, Nourbehesht N, Panichnantakul P, Holcatova I, *et al*: Loss of chromosome Y leads to down regulation of KDM5D and KDM6C epigenetic modifiers in clear cell renal cell carcinoma. Sci Rep 7: 44876, 2017.
31. Zhu M, Zhang RN, Zhang H, Qu CB, Zhang XC, Ren LX, Yang Z and Gu JF: PCGF6/MAX/KDM5D facilitates MAZ/CDK4 axis expression and pRCC progression by hypomethylation of the DNA promoter. Epigenetics Chromatin 16: 9, 2023.
32. Chen TM, Huang CM, Setiawan SA, Hsieh MS, Sheen CC and Yeh CT: KDM5D histone demethylase identifies platinum-tolerant head and neck cancer cells vulnerable to mitotic catastrophe. Int J Mol Sci 24: 5310, 2023.
33. Dunford A, Weinstock DM, Savova V, Schumacher SE, Cleary JP, Yoda A, Sullivan TJ, Hess JM, Gimelbrant AA, Beroukhim R, *et al*: Tumor-suppressor genes that escape from X-inactivation contribute to cancer sex bias. Nature Genet 49: 10-16, 2017.
34. Shen X, Hu K, Cheng G, Xu L, Chen Z, Du P and Zhuang Z: KDM5D inhibit epithelial-mesenchymal transition of gastric cancer through demethylation in the promoter of Cul4A in male. J Cell Biochem 120: 12247-12258, 2019.
35. Liu M and Gao N: KDM5D inhibits the transcriptional activation of FKBP4 by suppressing the expression of E2F1 in colorectal cancer in males. Biochem Pharmacol 194: 114814, 2021.
36. Li S, Wu Z, Li Q, Liang Q, Zhou H, Shi Y, Zhang R and Pan H: The prognostic value of AT-rich interaction domain (ARID) family members in patients with hepatocellular carcinoma. Evid Based Complement Alternat Med 2022: 1150390, 2022.
37. Duan Y, Du Y, Gu Z, Zheng X and Wang C: Expression, prognostic value, and functional mechanism of the KDM5 family in pancreatic cancer. Front Cell Dev Biol 10: 887385, 2022.
38. Abdel-Hafiz HA, Schafer JM, Chen X, Xiao T, Gauntner TD, Li Z and Theodorescu D: Y chromosome loss in cancer drives growth by evasion of adaptive immunity. Nature 619: 624-631, 2023.
39. Li J, Lan Z, Liao W, Horner JW, Xu X, Liu J, Yoshihama Y, Jiang S, Shim HS, Slotnik M, *et al*: Histone demethylase KDM5D upregulation drives sex differences in colon cancer. Nature 619: 632-639, 2023. Hannah J and Zhou P: Distinct and overlapping functions of the cullin E3 ligase scaffolding proteins CUL4A and CUL4B. Gene 573: 33-45, 2015.
40. Jin J, Arias EE, Chen J, Harper JW and Walter JC: A family of diverse Cul4-Ddb1-interacting proteins includes Cdt2, which is required for S phase destruction of the replication factor Cdt1. Mol Cell 23: 709-721, 2006.

41. Yasui K, Arii S, Zhao C, Imoto I, Ueda M, Nagai H, Emi M and Inazawa J: TFDP1, CUL4A, and CDC16 identified as targets for amplification at 13q34 in hepatocellular carcinomas. Hepatology 35: 1476-1484, 2002.
42. Jia L, Yan F, Cao W, Chen Z, Zheng H, Li H, Pan Y, Narula N, Ren X, Li H and Zhou P: Dysregulation of CUL4A and CUL4B Ubiquitin ligases in lung cancer. J Biol Chem 292: 2966-2978, 2017.
43. Hannah J and Zhou PB: The CUL4A ubiquitin ligase is a potential therapeutic target in skin cancer and other malignancies. Chin J Cancer 32: 478-482, 2013.
44. Chen LC, Manjeshwar S, Lu Y, Moore D, Ljung BM, Kuo WL, Dairkee SH, Wernick M, Collins C and Smith HS: The human homologue for the Caenorhabditis elegans cul-4 gene is amplified and overexpressed in primary breast cancers. Cancer Res 58: 3677-3683, 1998.
45. Hung MS, Mao JH, Xu Z, Yang CT, Yu JS, Harvard C, Lin YC, Bravo DT, Jablons DM and You L: Cul4A is an oncogene in malignant pleural mesothelioma. J Cell Mol Med 15: 350-358, 2011.
46. Ren S, Xu C, Cui Z, Yu Y, Xu W, Wang F, Lu J, Wei M, Lu X, Gao X, *et al*: Oncogenic CUL4A determines the response to thalidomide treatment in prostate cancer. J Mol Med (Berl) 90: 1121-1132, 2012.
47. Shiyanov P, Nag A and Raychaudhuri P: Cullin 4A associates with the UV-damaged DNA-binding protein DDB. J Biol Chem 274: 35309-35312, 1999.
48. Nag A, Bondar T, Shiv S and Raychaudhuri P: The xeroderma pigmentosum group E gene product DDB2 is a specific target of cullin 4A in mammalian cells. Mol Cell Biol 21: 6738-6747, 2001.
49. Kapetanaki MG, Guerrero-Santoro J, Bisi DC, Hsieh CL, Rapić-Otrin V and Levine AS: The DDB1-CUL4ADDB2 ubiquitin ligase is deficient in xeroderma pigmentosum group E and targets histone H2A at UV-damaged DNA sites. Proc Natl Acad Sci USA 103: 2588-2593, 2006.
50. Shinomiya T, Mori T, Ariyama Y, Sakabe T, Fukuda Y, Murakami Y, Nakamura Y and Inazawa J: Comparative genomic hybridization of squamous cell carcinoma of the esophagus: The possible involvement of the DP1 gene in the 13q34 amplicon. Genes Chromosomes Cancer 24: 337-344, 1999.
51. Dohna M, Reincke M, Mincheva A, Allolio B, Solinas-Toldo S and Lichter P: Adrenocortical carcinoma is characterized by a high frequency of chromosomal gains and high-level amplifications. Genes Chromosomes Cancer 28: 145-152, 2000.
52. Michiels EM, Weiss MM, Hoovers JM, Baak JP, Voûte PA, Baas F and Hermsen MA: Genetic alterations in childhood medulloblastoma analyzed by comparative genomic hybridization. J Pediatr Hematol Oncol 24: 205-210, 2002.
53. Englinger B, Mair M, Miklos W, Pirker C, Mohr T, van Schoonhoven S, Lötsch D, Körner W, Ferk F, Knasmüller S, *et al*: Loss of CUL4A expression is underlying cisplatin hypersensitivity in colorectal carcinoma cells with acquired trabectedin resistance. Br J Cancer 116: 489-500, 2017.
54. Ngan ES: Heterogeneity of neuroblastoma. Oncoscience 2: 837-838, 2015.
55. Louis CU and Shohet JM: Neuroblastoma: Molecular pathogenesis and therapy. Annu Rev Med 66: 49-63, 2015.
56. Nader JH, Bourgeois F, Bagatell R, Moreno L, Pearson ADJ and DuBois SG: Systematic review of clinical drug development activities for neuroblastoma from 2011 to 2020. Pediatr Blood Cancer 70: e30106, 2023.
57. Bedrnicek J, Vicha A, Jarosova M, Holzerova M, Cinatl J, Michaelis M, Cinatl J and Eckschlager T: Characterization of drug-resistant neuroblastoma cell lines by comparative genomic hybridization. Neoplasma 52: 415-419, 2005.
58. Procházka P, Libra A, Zemanová Z, Hřebačková J, Poljaková J, Hraběta J, Bunček M, Stiborová M and Eckschlager T: Mechanisms of ellipticine-mediated resistance in UKF-NB-4 neuroblastoma cells. Cancer Sci 103: 334-341, 2012.
59. Bachetti T, Di Paolo D, Di Lascio S, Mirisola V, Brignole C, Bellotti M, Caffa I, Ferraris C, Fiore M, Fornasari D, *et al*: PHOX2B-mediated regulation of ALK expression: In vitro identification of a functional relationship between two genes involved in neuroblastoma. PLoS One 5: e13108, 2010
60. Pfaffl MW, Horgan GW and Dempfle L: Relative expression software tool (REST) for group-wise comparison and statistical analysis of relative expression results in real-time PCR. Nucleic Acids Res 30: e36, 2002.
61. Kocak H, Ackermann S, Hero B, Kahlert Y, Oberthuer A, Juraeva D, Roels F, Theissen J, Westermann F, Deubzer H, *et al*: Hox-C9 activates the intrinsic pathway of apoptosis and is associated with spontaneous regression in neuroblastoma. Cell Death Dis 4: e586, 2013.
62. Su Z, Fang H, Hong H, Shi L, Zhang W, Zhang W, Zhang Y, Dong Z, Lancashire LJ, Bessarabova M, *et al*: An investigation of biomarkers derived from legacy microarray data for their utility in the RNA-seq era. Genome Biol 15: 523, 2014.
63. Oberthuer A, Berthold F, Warnat P, Hero B, Kahlert Y, Spitz R, Ernestus K, König R, Haas S, Eils R, *et al*: Customized oligonucleotide microarray gene expression-based classification of neuroblastoma patients outperforms current clinical risk stratification. J Clin Oncol 24: 5070-5078, 2006.
64. Wysocka J, Swigut T, Xiao H, Milne TA, Kwon SY, Landry J, Kauer M, Tackett AJ, Chait BT, Badenhorst P, *et al*: A PHD finger of NURF couples histone H3 lysine 4 trimethylation with chromatin remodelling. Nature 442: 86-90, 2006.
65. Li S, Shen L and Chen KN: Association between H3K4 methylation and cancer prognosis: A meta-analysis. Thoracic Cancer 9: 794-799, 2018.
66. Tumber A, Nuzzi A, Hookway ES, Hatch SB, Velupillai S, Johansson C, Kawamura A, Savitsky P, Yapp C, Szykowska A, *et al*: Potent and selective KDM5 inhibitor stops cellular demethylation of H3K4me3 at transcription start sites and proliferation of MM1S myeloma cells. Cell Chem Biol 24: 371-380, 2017.
67. Brodeur GM, Pritchard J, Berthold F, Carlsen NL, Castel V, Castelberry RP, De Bernardi B, Evans AE, Favrot M, Hedborg F, *et al*: Revisions of the international criteria for neuroblastoma diagnosis, staging and response to treatment. J Clin Oncol 11: 1466-1477, 1993.
68. Cheung NK, Kushner BH, LaQuaglia M, Kramer K, Gollamudi S, Heller G, Gerald W, Yeh S, Finn R, Larson SM, *et al*: N7: A novel multi-modality therapy of high-risk neuroblastoma in children diagnosed over 1 year of age. Med Pediatr Oncol 36: 227-230, 2001.
69. Haupt S, Caramia F, Klein SL, Rubin JB and Haupt Y: Sex disparities matter in cancer development and therapy. Nat Rev Cancer 21: 393-407, 2021.
70. Hollows R, Wei W, Cazier JB, Mehanna H, Parry G, Halford G and Murray P: Association between loss of Y chromosome and poor prognosis in male head and neck squamous cell carcinoma. Head Neck 41: 993-1006, 2019.
71. Huang RS, Kistner EO, Bleibel WK, Shukla SJ and Dolan ME: Effect of population and gender on chemotherapeutic agent-induced cytotoxicity. Mol Cancer Ther 6: 31-36, 2007.